CLARA: Capacity Loss-Aware Resource Assignment Algorithm for Translucent SDM EONs

Shrinivas Petale, Suresh Subramaniam
Department of Electrical and Computer Engineering, The George Washington University, Washington, DC, USA
{*srpetale,suresh*}*@gwu.edu*

***Abstract*—Space division multiplexed elastic optical networks (SDM-EONs) offer increased fiber capacity to enhance service provisioning with the help of fine-grained flexible spectrum, multiple spatial modes, and efficient modulation formats. The connection resource provisioning problem in SDM EONs is the route, modulation format (MF), core and spectrum assignment (RMCSA) problem. The intercore crosstalk (XT) between ongoing connections on adjacent cores degrades the signal transmission and thus needs to be handled properly while assigning resources. The use of multiefficient MFs in translucent optical networks poses a challenge of balancing the spectrum utilization and XT accumulation in the network. In this paper, we propose an RMCSA algorithm called as Capacity Loss Aware Resource Assignment Algorithm (CLARA) which optimizes the utilization of network capacity to improve resource availability and thus network performance. Extensive simulation experiments indicate that CLARA significantly reduces the bandwidth blocking probability and improves resource utilization in a variety of scenarios. It is observed that it balances the spectrum utilization and XT accumulation more efficiently as compared to algorithms in the literature.**

***Index Terms*—SDM EON; Intercore crosstalk; RMCSA; Multicore fiber; Capacity loss; Translucent optical network.**

2023 IEEE Future Networks World Forum (FNWF) | 979-8-3503-2458-7/23/$31.00 ©2023 IEEE | DOI: 10.1109/FNWF58287.2023.10520496

I. Introduction

5G networks are expected to cause an explosive increase in data traffic and services which demand flexible, high capacity and low latency reliable optical transport networks. Recent advancements show that elastic optical networks (EONs) with the support of space division multiplexing (SDM) can fulfill this requirement [1]. In EON, the spectrum is divided into small grids to offer flexible spectrum choices. The set of spectrum slices are assigned to the requests in the form of a superchannel for transmission. SDM technology allows parallel transmission of signals in the same fiber through multiple cores, called as multicore fibers (MCFs). Thus the combination of SDM and EON technologies result in space division multiplexed elastic optical networks (SDM-EONs) which offer huge capacity to mitigate the problem of capacity crunch [1], [2].

The parallel transmission of signals though spatial modes results in inter-core crosstalk (XT) between the signals which degrades the quality of transmission (QoT). Regenerators in translucent SDM-EON increases the use of spectrally efficient but highly XT-sensitive modulation formats (MFs). Such selections increases the XT accumulation in the network which prevent resources from being utilized efficiently. The degradation of QoT below the threshold leads to incomplete reception and thus dropping of connections [3]. The important problem of resource selection is the route, MF, core and spectrum assignment (RMCSA) problem in translucent optical networks. The complexity of RMCSA increases due to XT between signal transmissions through MCFs [4].

Various approaches of considering XT in RMCSA are possible to increase the efficiency of network performance – such as XT avoidance or XT aware approaches [5]. The use of a significant value of XT threshold can ease the complexity of RMCSA [6]. Further, multiple candidate shortest paths help reduce the XT levels in the network [7]. However, these approaches alone cannot increase the efficiency of the network. It is necessary to use a XT-based approach to select the resources to not only handle the XT but also improve the resource utilization.

In this paper, we solve the RMCSA problem with the help of an efficient RMCSA algorithm called as Capacity Loss Aware Resource Assignment algorithm (CLARA) for translucent SDM EON. As the name suggests, it improves the selection of resources so as to minimize the loss in network capacity which in turn leaves more resources for future connection requests. CLARA accounts for XT while calculating the loss in capacity to efficiently select the resources. It handles spectrum utilization and XT accumulation in the network by selecting MF, core and spectrum for the arriving lightpath requests in an efficient manner.

The paper is organized as follows. The network model and problem statement are introduced in Section II. Definitions and details of the CLARA algorithm are presented in Sections III and IV. Section V presents simulation results. Finally, the paper is concluded in Section VI.

II. Network Model and Problem Statement

Here we explain the network model used in this paper and the problem statement. The symbols used in this paper are given in Tab. I. We assume that the SDM-EON operates with a flexible grid of 12.5 GHz granularity and is equipped with coherent transceivers (TRXs). The TRXs support reconfigurable bit-rates and various MFs. The TRXs operate at a fixed baud rate of 14 GBaud, and each TRX transmits/receives an optical carrier allocated on 2 frequency slices (FSs) (i.e., 25 GHz). If the requested bit-rate exceeds the maximum capacity of a single TRX using a particular MF, the request is carried by several optical carriers within one superchannel (SCh). Each SCh is separated from neighbor SChs by 12.5 GHz guard-bands. The nodes are connected using optical links consisting of MCFs. Each fiber link consists of the same set of MCFs with a specified

core geometry in both the directions.[1] Two widely considered core geometries, 3-core and 7-core [8], are studied. The effect of XT is dominant between the cores that are right next to each other called as *adjacent/neighbor cores*. For instance, each core in a 3-core fiber has two adjacent cores. Similarly, in 7-core fiber, the outer cores have three adjacent cores and the center core has six adjacent cores (see Fig. 1). Furthermore, spatial continuity is imposed which means that the same core is assigned to a lightpath on all MCF links on a route. Lightpath requests arrive at a specified Poisson rate with exponentially distributed mean holding time of unity (arbitrary units) and the datarates are uniformly distributed over a given range.

In a given network topology, 20-30% of the nodes are assumed to have regeneration capabilities. Regenerators are placed at nodes with higher nodal degrees.[2] Regenerators break up a single long lightpath into multiple shorter transparent segments and thereby enable the use of higher MFs. We consider two variants of regenerator capabilities. The first variant is when the regenerator can also perform modulation and spectrum conversion and the second variant is when it cannot perform either. The XT model of [9] is used to obtain the transmission reaches (TRs) for various MFs and for various values of lit adjacent cores (or litcores for short), as shown in Table II (from [10]). We consider average XT values of -25 dB [11] and -40 dB between two adjacent cores after a single span of propagation [10]. The total XT experienced by a core is the sum of individual average XT contributions from each neighbor. The number of allowable lit cores is denoted as γ. The γ for MF of an existing connection on a core decides the allowable occupancy of adjacent cores on the overlapping spectrum (OS); thus a high value of γ is desired. For an incoming connection request, γ of candidate MF decides whether the spectrum can be occupied with this MF based on occupancy of OS on adjacent cores. With an increase in γ value, the XT level experienced by the core increases resulting in shorter TRs. Hence, for a longer path if a higher MF is chosen, the γ value will be low. Thus, although a higher MF saves spectrum, it blocks the occupancy of OS on adjacent cores. For the same path if a lower MF is chosen, more spectrum will be required but the OS on adjacent cores will be allowed to be occupied due to larger γ. The objective of our RMCSA problem is to decrease the bandwidth blocking probability (BBP) by maintaining a proper balance between spectrum utilization and XT level.

III. Network Capacity and Capacity Loss

In this section, we define various quantities that are used in CLARA. We also present an example to illustrate how these are computed in a translucent network. A detailed explanation of the computation of these quantities for transparent networks is presented in our recent work in [12], [13]. We call a set of FSs as a slice window (SW). The aim of CLARA is to choose the best SW along with the MF and core to yield the best blocking performance. On shortest path k of route r, namely r^k, there are a number of SWs, with the first one having starting FS of 1, the second SW with starting FS of 2, and so on. The *capacity* and *capacity loss (CL)* of a candidate SW are defined as follows.

[1]In this paper, we assume that all the links have a single MCF in each direction, but the proposed work can be easily generalized for multiple fibers per link.

[2]The focus of this paper is on the RMCSA problem and not on regenerator placement. We use this simple method to place the given regenerators.

Table I: Symbols and notations.

Symbol	Definition
N	Number of nodes in the network
L	Number of links in the network
D	Set of digital modulation formats $\{f_1, f_2, \ldots, f_{\lvert D\rvert}\}$
C	Number of cores per fiber
K	Number of shortest paths considered for a route
Bw	Total spectrum available in GHz
δ	Slice width in GHz
g_b	Number of guard bands of size δ GHz
S	Total number of frequency slots available
r	Arbitrary route
k	Arbitrary candidate path
e	Arbitrary network link
r^k	k^{th} shortest path on route r
M	Set of connection sizes $\{m_1, m_2, \ldots, m_{\lvert M\rvert}\}$
m_i	i^{th} datarate in Gbps

A. Capacity of an SW

The capacity of the n^{th} SW on r^k for a given MF f_d, denoted by $\upsilon_n^{k,d}$, is the number of cores on the whole path on which the SW can be assigned in the current network state (i.e., before resource assignment for the incoming request). Here, the current network state includes the litcore restriction of the already established connections on OS on adjacent cores. When SW is assigned to the incoming request on a core with MF f_d, the capacity would decrease by an amount that depends on f_d and its corresponding allowable γ for the length of the lightpath. Thus, the remaining capacity of the n^{th} SW on c^{th} core on r^k using f_d, denoted as $\upsilon_{n,c}^{'k,d}$, is the capacity of the SW *if it were to be assigned to the incoming request*, with the actual value of γ of selected MF f_d, denoted as γ_d, and the actual network state.

B. Capacity Loss of a Slice Window

The remaining capacity of a SW after the resource assignment of a connection varies based on the selected core and XT tolerance of the selected MF f_d. Thus, for every core and MF pair, $\upsilon_{n,c}^{'k,d}$ varies. In this paper, we calculate the capacity loss (CL) for every SW based on the hypothetical assignment of the core, MF, and SW for the incoming request. The decrease in capacity after the hypothetical provisioning from the capacity before provisioning gives the total CL. If the XT constraints are removed, CL for a particular selection of SW for a core on a route is one. However in SDM EON, the XT tolerance of the selected MF on a core decides the future occupancy on adjacent cores, thus the CL can be more than one. Finally, the CL for the n^{th} SW on c^{th} core on r^k using f_d is calculated using (1).

$$\psi_{n,c}^{k,d} = \upsilon_n^{k,d} - \upsilon_{n,c}^{'k,d}. \tag{1}$$

The optimal choice of spectrum is when shared resources in the network are still available for future demands. When an SW on a path is assigned to a request, there is a CL for the

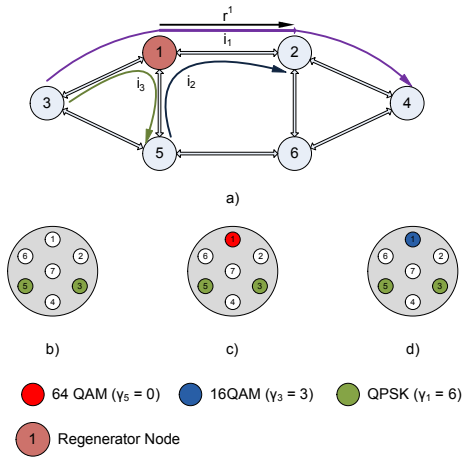

Figure 1: Effect of selection of two different MFs on capacity.

SW on all the overlapping (shared) paths as well. Thus, we consider the network occupancy by calculating the CL of the same SW on all the shared paths. Let, Z^k be the set of all the shared paths; $Z^k = i_1, i_2, \ldots, i_z$. Suppose that the incoming request has datarate m and arrived on route r, and is denoted by $\Delta(r, m)$. The number of FSs required to accommodate datarate m using MF f_d is denoted as β_d^m. We assume a lightpath tuple, $l_{\Delta(r,m)}(k, c, n, \beta_d^m)$, which represents the n^{th} SW of size β_d^m on c^{th} core on r^k for request $\Delta(r, m)$. The total CL of $l_{\Delta(r,m)}(k, c, n, \beta_d^m)$ is shown in (2); where, $\psi^{r\,k,d}_{n,c}$ is the CL ($\psi^{k,d}_{n,c}$) on r^k and $\psi^{i\,z,d}_{n,c}$ is the CL ($\psi^{k,d}_{n,c}$) on the z^{th} shared path i_z ($i_z \in Z^k$).

$$\psi'(l_{\Delta(r,m)}) = \psi^{r\,k,d}_{n,c} + \sum_{z=1}^{|Z^k|} \psi^{i\,z,d}_{n,c}. \tag{2}$$

Based on the presence of the regenerator on an intermediate node, the route r^k is divided into lightpath segments where the i^{th} segment is denoted as s_i. The above calculations can be repeated for each segment separately until the resources on all the segments is obtained. If no regenerator is present on r^k then s_1 and r^k are the same.

C. An Illustrative Example

Table II: Transmission reaches of MFs for different values of allowable lit core (γ) from Table II in [10].

	Modulation Formats ($\|D\| = 5$, $f_d \in D$)				
γ **(Litcores)**	**QPSK**	**8 QAM**	**16 QAM**	**32 QAM**	**64 QAM**
0	9050	3600	1950	1000	500
1	1350	500	250	150	50
2	700	250	150	50	0
3	450	200	100	50	0
4	350	150	50	0	0
5	300	100	50	0	0
6	250	100	50	0	0

We illustrate the calculations of CL for the first SW (n = 1) on core 1 of a 7-core fiber for two different candidate MFs on the main route in the presence of regenerator with the help of an example shown in Fig. 1 and Table II. Here, D is the set of MFs $\{f_1, f_2, \ldots, f_{|D|}\}$. In this example, we assume that $|D|$ = 5 and use 64 QAM (f_5) and 16 QAM (f_3) for the explanation. We use Table II to get γ_d of both the MFs. Table II reports the TRs calculated for the combination of MF and number of adjacent litcores (γ) for the TRX baudrate of 14 GBaud and XT threshold (XT^{th}) of -25 dB. The number of litcores varies from 0 to 6 in a 7-core fiber, thus TRs are given for each MF for γ = 0, ..., 6. The corresponding value of γ for which the TR of an MF is greater than or equal to the path length is chosen as γ_d for a given MF on this path.

In Fig. 1a, a six node topology is shown with a regenerator at node 1. Three shortest paths (SPs) from different source and destinations are shown and denoted as i_1 (3-1-2), i_2 (5-1-2) and i_3 (3-1-5). Here, in the abscence of regenerator, only i_1 and i_2 share a link (between nodes 1 and 2) with r^1; thus, these two SPs will be considered in the CL calculations i.e., $Z^1 = \{i_1, i_2\}$. As node 1 has regenerator, the SPs will be broken down into lightpath segments. Here, i_1 and i_2 are broken down into $i_1^{s_1}$ (3-1) and $i_1^{s_2}$ (2-3), and $i_2^{s_1}$ (5-1) and $i_2^{s_2}$ (1-2). Thus the updated Z^1 is $Z^1 = \{i_1^{s_2}, i_2^{s_2}\}$. The CL of a given SW is calculated on r^1, $i_1^{s_2}$ and $i_2^{s_2}$ to get final CL.

The occupancy of cores on r^1 is shown in Fig. 1a. Suppose that the first 20 FSs out of S = 320 FSs on cores 3 and 5 are occupied by a connection which uses QPSK (f_1) with γ_1=6, and the FSs on the other cores are free as shown in Fig. 1b. We assume that the spectrum on all the cores on rest of the links is vacant. Suppose a connection request of 120 Gb/s arrives on r, and the length of r^1 is 54 km which requires β_5^m=2 FSs, β_3^m=5 FSs and β_1^m=7 FSs when 64 QAM (f_5), 16 QAM (f_3) and QPSK (f_1) are chosen. The first SW (n=1) for 64 QAM is of size β_5^m FSs and for 16 QAM is of size β_3^m. In both the cases, the SW of respective sizes is free on cores 1, 2, 4, 6 and 7, i.e., the capacity before any assignment in both the cases is 5, i.e., $\upsilon_1^{1,5}$=$\upsilon_1^{1,3}$=5. The hypothetical assignment is done to see the remaining capacity after a selection of the MF. Starting from the highest MF, i.e., 64 QAM (f_5), the hypothetical assignment is done on core 1 as shown in Fig. 1c. From Table II for 64 QAM, as the first TR, searched from the bottom to the top, at γ=0 (500 Km) is higher than path length (54 Km), γ_5 is set to 0. It means that based on XT tolerance of 64 QAM, if assigned for the current connection on core 1, the connection will not allow adjacent cores 2, 6, and 7 to be assigned to future requests on the OS as long as it exists in the network. Thus, OS only on core 4 will be available for future connections, which means that the capacity after hypothetical assignment with 64 QAM is 1, i.e., $\upsilon_{1,1}^{'1,5}$=1. Thus using (1), CL $\psi^{r\,1,5}_{1,1}$ in this case is $\upsilon_1^{1,5} - \upsilon_{1,1}^{'1,5}$=5-1=4.

Similarly, the CL on $i_2^{s_2}$, $\psi^{i\,2,5}_{1,1}$, is 4 as it also has only link between nodes 1 and 2. As the spectrum on link between nodes 2 and 4 is assumed to be vacant, the CL on $i_1^{s_2}$, $\psi^{i\,1,5}_{1,1}$, is also 4 due to imposed spatial continuity constraint. Because, when spatial continuity is imposed, the first 20 FSs on cores 3 and 5 on the link between nodes 2 and 4 are marked as unusable, which leads to same capacity before and after hypothetical assignment of respective MF. Thus, using (2), the total CL ($\psi^{'}(l_{\Delta(r,m)})$) with 64 QAM is 4+4+4=12.

Similarly, for the first SW of size β_3^m with 16 QAM, from

Table II, we get γ_3=3, i.e., if assigned, it will allow the OS to occupy on the adjacent cores 2, 6 and 7 by future requests as long as it remains in the network. Thus, OS on cores 2, 4, 6, and 7 will be available for future connections. Thus, the capacity after hypothetical assignment with 16 QAM is 4, i.e., $\upsilon_{1,1}^{'1,3}$=4. Thus CL $\psi^{r}{}_{1,1}^{1,3}$ in this case is $\upsilon_1^{1,3} - \upsilon_{1,1}^{'1,3}$=5-4=1. Similarly, CL on $i_2^{s_2}$, $\psi^{i}{}_{1,1}^{2,3}$, is 1. Due to spatial continuity constraint, the CL at $i_1^{s_2}$, i.e., $\psi^{i}{}_{1,1}^{1,3}$ is 1. Thus, the total CL ($\psi^{'}(l_{\Delta(r,m)})$) with 16 QAM is 1+1+1=3.

IV. Capacity Loss-Aware Resource Assignment (CLARA)

We now describe our proposed CLARA algorithm by considering two variants of regenerators - one which performs modulation and spectrum conversion and another which does not allow either. The second case can be seen as a special case of the first, so we explain the CLARA algorithm for the first variant. First, we define an available SW (which is a candidate SW for assignment).

Definition IV.1 (Available Slice Window)**.** An SW of size β_d^m is called *available SW* for assignment to a connection request with datarate m on route r, denoted as $\Delta(r,m)$, using MF f_d on core c on all the links on a given SP of route r $\iff$ all the FSs from index n to n+$\beta_d^m - 1$, on the core c on all the links of given SP of route r, a) are free, i.e., not assigned to any other connection, b) can accommodate $\Delta(r,m)$ without affecting ongoing connections on OS on adjacent cores of core c, and c) can accommodate $\Delta(r,m)$ based on XT sensitivity of MF f_d.

All the possible SWs of spectrum for datarate m using MF f_d on all the cores are stored in set B_d^m. For datarate m, H^m is the set of all B_d^m sets for all MFs. The SW of index n on core c in B_d^m is denoted by $b_{c,n}^{m,d}$. For the datarate m, V^m is the set of β_d^m for all MFs. For the datarate m, the MFs in D are sorted in D^m based on spectrum requirement. If two or more MFs have the same spectrum requirements then the lowest among them is considered as candidate MF and all such MFs are stored in D^m.

The selection of a path, MF, core, and SW by CLARA for a lightpath is explained in Algorithm 1. The TR of MF f_d for the corresponding value of γ is denoted as T_d^γ. The optimal lightpath $l^*_{\Delta(c,m)}(k^*, c^*, n^*, \beta^*)$, its corresponding CL, index of SP and number of processed lightpath segments, denoted as PLS, are initialized in Line 1. Assume that the k^{th} SP is broken down into one or more LSs and are stored in Ω_r^k; where i^{th} LS is denoted as s_i. Here, the desired path index, core index, index of SW and demandsize are denoted by k^*, c^*, n^*, and β^*. In Line 2, the algorithm continues until either the SW with the lowest (best) CL is found or the search over all the SPs is completed. In Line 3, the search is done for each lightpath segment s_i in Ω_r^k. For a given s_i, the search is initiated for those MFs whose maximum TR, i.e., TR without the consideration of XT at $\gamma = 0$ (T_d^0) is higher than path length of the k^{th} SP in Line 4. In Line 5, the allowable litcore value γ_d is the γ value for which the TR value T_d^γ is greater than or equal to the path length of the k^{th} SP. In Line 6, the actual size of SW is obtained. In Line 7, loop iterating over all the choices of SWs in B_d^m is started. The candidate lightpath on segment s_i, denoted as l^{k,s_i} is initiated in Line 8. If the SW is available as per definition, the CL is calculated for the current SW $b_{c,n}^{m,d}$ on lightpath l^{k,s_i} in Line 10. In Lines 11-13, the information of SW which offers the least value of CL is stored as the desired lightpath l^{*k,s_i}. In Line 18, the algorithm checks whether the desired resources are available on all the lightpath segments or not. If these are obtained then the algorithm saves the information of selected resources on all the segments into the optimal lightpath l^* and stops. Otherwise, the algorithm continues with the next SP in Line 21-23. Finally, after all the SWs on all the cores on the whole path are processed, the optimal lightpath $l^*_{\Delta(r,m)}$ is selected for a given connection, and the network resources are assigned to the connection request accordingly. If an SW is not found on any of the SPs (i.e., $l^*_{\Delta(r,m)} = \varnothing$), the request is rejected.

Algorithm 1 CLARA Algorithm

Input: Network topology, $\Delta(r,m)$, set of SPs $P(r)$, set of LSs Ω_r^k and their lengths w^{s_i} and, D^m, V^m, H^m, S

Output: $l^*_{\Delta(r,m)}(k^*, c^*, n^*, \beta^*)$

1: $l^*_{\Delta(r,m)} \leftarrow \varnothing$, $\psi'(l^*_{\Delta(r,m)}) \leftarrow \infty$, $k \leftarrow 1$, PLS $\leftarrow 0$
2: **while** $l^*_{\Delta(r,m)} = \varnothing \wedge k \neq K$ **do**
3: **for all** $s_i \in \Omega_r^k$, $\Omega_r^k \in P(r)$ **do**
4: **for all** ($f_d \in D^m \wedge T_d^0 \geq w^{s_i}$) **do**
5: Get lit core $\gamma_d \leftarrow \gamma$ for which $T_d^\gamma \geq w^{s_i}$
6: Get β_d^m from V^m
7: **for all** $b_{n,c}^{m,d} \in B_d^m$; $B_d^m \in H^m$ **do**
8: Get candidate lightpath $l^{k,s_i}_{\Delta(r,m)} \leftarrow (s_i, c, n, \beta_d^m)$
9: **if** SW is *available* **then**
10: Calculate CL $\psi'(l^{k,s_i}_{\Delta(r,m)})$ of $b_{n,c}^{m,d}$ SW
11: **if** $\psi'(l^{k,s_i}_{\Delta(r,m)}) < \psi'(l^{*k,s_i}_{\Delta(r,m)})$ **then**
12: $l^{*k,s_i}_{\Delta(r,m)} \leftarrow l^{k,s_i}_{\Delta(r,m)}$, $c^{*s_i} \leftarrow c$, $n^{*s_i} \leftarrow n$, $\beta^{*s_i} \leftarrow \beta_d^m$, PLS $\leftarrow$ PLS + 1
13: **end if**
14: **end if**
15: **end for**
16: **end for**
17: **end for**
18: **if** PLS = $|\Omega_r^k|$ **then**
19: $l^*_{\Delta(r,m)} \leftarrow \left\{l^{*k,s_i}_{\Delta(r,m)} \mid \forall\ s_i \in \Omega_r^k\right\}$, $c^* \leftarrow \left\{c^{*s_i} \mid \forall\ s_i \in \Omega_r^k\right\}$, $n^* \leftarrow \left\{n^{*s_i} \mid \forall\ s_i \in \Omega_r^k\right\}$, $\beta^* \leftarrow \left\{\beta^{*s_i} \mid \forall\ s_i \in \Omega_r^k\right\}$, $k^* \leftarrow k$
20: **break**
21: **else**
22: $k \leftarrow k+1$, PLS $\leftarrow 0$
23: **end if**
24: **end while**

V. Simulation Results

We now present simulation results comparing CLARA with several other algorithms for a variety of scenarios. We use

two practical topologies: generic German (DT) and European (EURO) shown in [12]. The spectrum of 4 THz (Bw = 4000) is considered on each link with each slice of 12.5 GHz (δ = 12.5) i.e., 320 FSs (S = 320). Poisson connection arrival process with exponentially distributed holding time of 1 (arbitrary time unit) is assumed. The Erlang loads were chosen so that the BBP values generally range between 10^{-5} and 10^{-1}. A total of 100,000 requests are generated per trial, with the first 10,000 warm up requests being discarded. 95% confidence intervals are obtained for 10 trials in each experiment. The data rates are uniformly distributed between 40-400 Gbps with the granularity of 40 Gbps. There exist 3 SPs between every s-d pair (K = 3). Total of five MFs ($|D|$ = 5), i.e., f_1 to f_5 are used viz., QPSK, 8 QAM, 16 QAM, 32 QAM and 64 QAM. The TR model for each MF with the XT per span of -25 dB and -40 dB with 14 GBaud TRX with the span length of 50 km is used from [10]. 20-30% of the nodes i.e., three nodes in DT topology and five nodes in EURO topology from higher to lower nodal degree are assumed to have regeneration capabilities.

We compare the performance of CLARA with a baseline XT-aware first fit algorithm (xtFF) [5], XT avoid approach (XA) [5], first fit with worst case XT consideration (WF) [5], [8], [14] and KCAP [15]. xtFF chooses the highest MF and the first available SW for assignment. XA chooses MF by first fit policy and core and spectrum to avoid XT. WF chooses MF and core with first fit policy but the TR model for each core considers worst case scenario that all the adjacent cores are occupied. KCAP is a path priority-based core and spectrum assignment algorithm. The cores are divided into groups and the path-core pairs are searched in the increasing order of required FSs which are obtained using TR model for every group. The algorithms are compared for the same parameters; especially, for the same XT^{th}, with imposed spatial continuity constraint, and spectrum choices available for spectrum search. The KSP routing is used with these algorithms. The transmission reach model for a given XT^{th} value is the same for all the algorithms.

The variation in BBP, and corresponding utilized MFs and SPs when regenerators can perform modulation and spectrum conversion are shown in Fig. 2 and Fig. 3. Similar results when modulation and spectrum conversion are not allowed are shown in Fig. 4 for same loads. In Fig. 3 and Fig. 4, the first set of five bars for each algorithm indicate the % utilization of MFs, mentioned as ':MF', and the second set of five bars indicate the % utilization of SPs, mentioned as ':SP'.

In Fig. 2a and 2b, the performance of CLARA for XT^{th}=-25dB and C=3 is shown for both the topologies. CLARA outperforms the other algorithms. The performance of KCAP is better in DT but not in EURO as compared to other algorithms because of longer path lengths in EURO and restrictive TR model. Longer path lengths are the outcome of longer link lengths, which affect the sorting of SPs due to minor difference between path lengths and TRs for XT^{th} of -25dB. WF and KCAP have similar use of TR model based on number of adjacent cores. However, due to offline sorting of SPs based on spectrum requirement in KCAP, it always performs better than WC. XA assigns resources using first fit policy and by avoiding the XT which in turn leaves fewer choices of spectrum. xtFF on the other hand uses a XT-aware approach which improves its performance over XA. Similarly, CLARA outperforms all algorithms for the XT^{th} of -40dB and C = 7 as shown in Fig. 2c and Fig. 2d. Here the performance of KCAP does not degrade in EURO due to the more relaxed TR model. The performance of CLARA is consistently better as the selection of resources involves the consideration of XT such that the effect on the network capacity is least. The difference in performance of different algorithms occurs due to variation in selection of MFs in different scenarios. It is clear from the distributions that selecting only the highest MF cannot be a better approach in SDM-EON. In case of XT^{th} of -25dB and C = 3, selection of lower MFs improves the performance as shown in Fig. 3a and Fig. 3b. It also happen because the XT effects with the selection of higher MFs is higher due to the restrictive TR model whereas selection of lower MFs increases the choices of *available* SWs. However, for a more flexible TR model in case of XT^{th} of -40dB and C = 7, equally uniform selection of MFs is a better approach as done by CLARA as shown in Fig. 3c and Fig. 3d.

The utilization of SPs in Fig. 3 shows how current selection of resources affects the availability of resources for future connections. In all the cases, CLARA assigns resources to connections on the first SP while other algorithms use the second and third SPs due to unavailability of resources on the first SP. In other words, if the number of SPs between each s-d pair is reduced to 1 from 3, the performance of CLARA will remain unaffected while the other algorithms will block more requests.

Results when modulation and spectrum conversion are not allowed at regenerator node for XT^{th} of -25dB and C = 3 are shown for DT in Fig. 4a, and XT^{th} of -40dB and C = 7 for EURO in Fig. 4b for the same loads used in Fig. 2a and Fig. 2d. The corresponding utilization of MFs and SPs are shown in Fig. 4c and Fig. 4d. Once again, we see that CLARA outperforms the other algorithms. However, there is a change in performance due to utilized MFs and SPs. This shows that a minor variation in the selection pattern of MFs and selected MFs can significantly change the network performance. It is evident from the performance evaluation that CLARA efficiently selects resources (MF, core and SW) for different core geometries and path lengths in different topologies.

VI. Conclusion

We addressed the dynamic RMCSA problem in space division multiplexed elastic optical networks. We proposed an RMCSA algorithm called Capacity Loss-Aware Resource Allocation Algorithm (CLARA) which considers inter-core crosstalk while selecting network resources. CLARA achieves a good balance between spectrum utilization and crosstalk levels in the network. It considers network occupancy to calculate the capacity loss and select the slice window which has the least effect on the network for future connections. Extensive simulation results show the vastly improved performance of CLARA over algorithms in the literature.

Acknowledgement This work was supported in part by NSF grants CNS-1813617 and CNS-1818858.

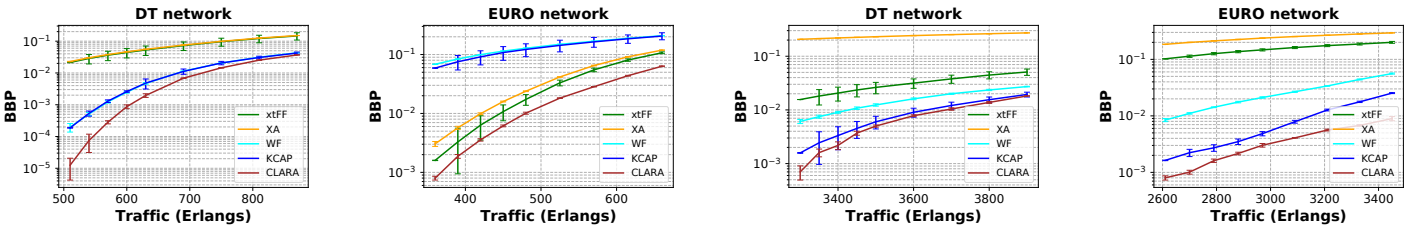

(a) XT^{th} = -25dB, C = 3 (b) XT^{th} = -25dB, C = 3 (c) XT^{th} = -40dB, C = 7 (d) XT^{th} = -40dB, C = 7

Figure 2: Variation in BBP wrt traffic for different XT^{th} values, C values and topologies when modulation and frequency conversions are allowed at regenerator node.

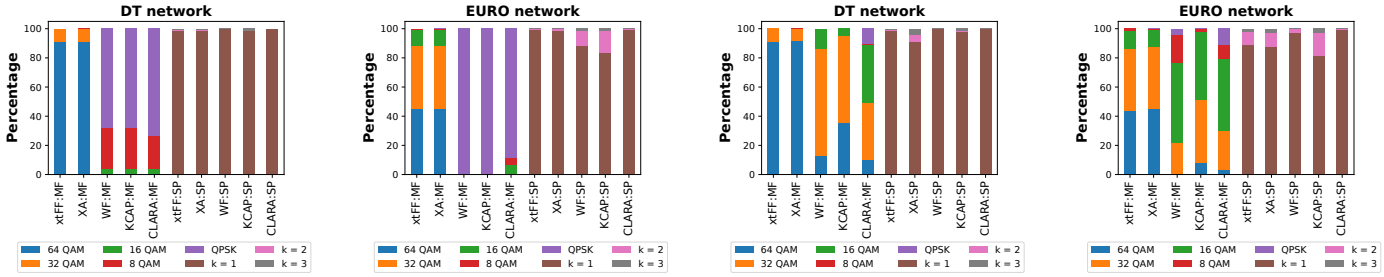

(a) XT^{th} = -25dB, C = 3 (b) XT^{th} = -25dB, C = 3 (c) XT^{th} = -40dB, C = 7 (d) XT^{th} = -40dB, C = 7

Figure 3: Distribution of utilized MFs and SPs for different XT^{th} values, C values and topologies when modulation and frequency conversions are allowed at regenerator node.

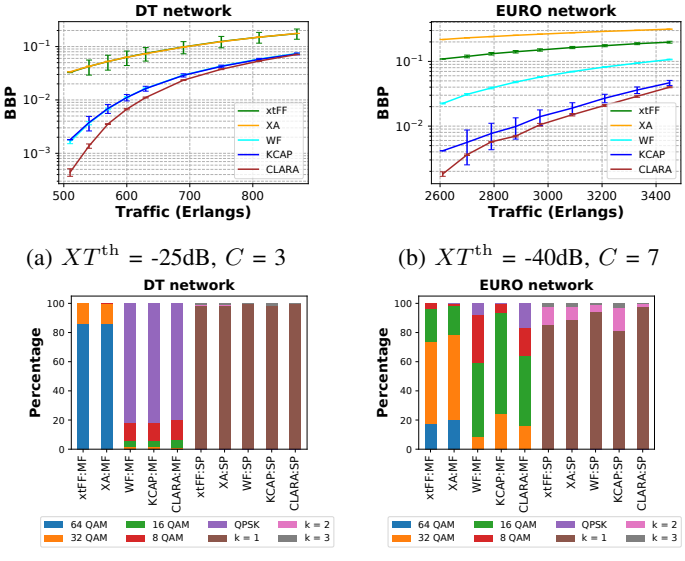

(a) XT^{th} = -25dB, C = 3 (b) XT^{th} = -40dB, C = 7

(c) XT^{th} = -25dB, C = 3 (d) XT^{th} = -40dB, C = 7

Figure 4: Distribution of utilized MFs and SPs for different XT^{th} values, C values and topologies when modulation and frequency conversions are not allowed at regenerator node.

REFERENCES

[1] Brasileiro et al., "A survey on challenges of spatial division multiplexing enabled elastic optical networks," Opt. Switch. Netw., p. 100584, 2020.

[2] Saridis et al., "Survey and evaluation of space division multiplexing: From technologies to optical networks," IEEE Commun. Surv. Tutor., vol. 17, no. 4, pp. 2136–2156, 2015.

[3] Arpanaei et al. "Three-dimensional resource allocation in space division multiplexing elastic optical networks." J. Opt. Commun. Netw. 10.12 (2018): 959-974.

[4] Walkowiak et al., "Effective worst-case crosstalk estimation for dynamic translucent SDM elastic optical networks," Proc. ICC 2019.

[5] Yang et al., "Routing, spectrum, and core assignment in sdm-eons with mcf: node-arc ilp/milp methods and an efficient xt-aware heuristic algorithm," J. Opt. Commun. Netw., vol. 10, no. 3, pp. 195–208, 2018.

[6] Zhang et al., "Anycast planning in space division multiplexing elastic optical networks with multi-core fibers," IEEE Commun. Lett., vol. 20, no. 10, pp. 1983–1986, 2016.

[7] Oliveira et al., "Multipath routing, spectrum and core allocation in protected sdm elastic optical networks," Proc. GLOBECOM 2019.

[8] Klinkowski et al., "Dynamic crosstalk-aware lightpath provisioning in spectrally-spatially flexible optical networks," J. Opt. Commun. Netw., vol. 11, no. 5, pp. 213–225, 2019.

[9] Poggiolini et al., "The gn model of non-linear propagation in uncompensated coherent optical systems," J. Light. Technol., vol. 30, no. 24, pp. 3857–3879, 2012.

[10] Rottondi et al., "Crosstalk- aware core and spectrum assignment in a multicore optical link with flexible grid," IEEE Trans Commun, vol. 67, no. 3, pp. 2144–2156, 2018.

[11] Sakaguchi et al., "305 tb/s space division multiplexed transmission using homogeneous 19-core fiber," J. Light. Technol., vol. 31, no. 4, pp. 554–562, 2012.

[12] Petale et al., "TRA: an efficient dynamic resource assignment algorithm for MCF-based SS-FONs," J. Opt. Commun. Netw., vol. 14, no. 7, pp. 511–523, 2022.

[13] Petale et al., "Tridental resource assignment algorithm for spectrally-spatially flexible optical networks," Proc. ICC 2021.

[14] Fujii et al., "On-demand spectrum and core allocation for reducing crosstalk in multicore fibers in elastic optical networks," J. Opt. Commun. Netw., vol. 6, no. 12, pp. 1059–1071, 2014.

[15] Agrawal et al., "Core arrangement based spectrum- efficient path selection in core-continuity constrained ss-fons," Proc. ONDM 2019.